

Shear Effect in Beta-Phase Induction of Polypropylene in a Single Screw Extruder

Fabiola Navarro-Pardo,¹ Julio Laria,² Tomas Lozano,¹ Ana B. Morales-Cepeda,¹ Pierre G. Lafleur,³ Saul Sánchez-Valdés,⁴ Francisco Rodríguez-González⁴

¹División de Estudios de Posgrado e Investigación, Instituto Tecnológico de Cd. Madero, Juventino Rosas y Jesús Urueta, Col. Los Mangos, C.P. 89440, Cd. Madero, Tamaulipas, México

²Universidad Autónoma de Tamaulipas, Facultad de Ingeniería "Arturo Narro Siller", Centro Universitario Tampico-Madero, C.P. 89000, Tampico, Tamaulipas, México

³Department of Chemical Engineering, École Polytechnique de Montréal, Stn Centre-Ville, Montreal, Quebec H3C 3A7, Canada

⁴Centro de Investigación en Química Aplicada (CIQA). Blvd Enrique Reyna No. 140, C.P. 25100, Saltillo, Coahuila, México

Correspondence to: T. Lozano (E-mail: tomas.lozano@polymtl.ca)

ABSTRACT: In this work, we investigated the effect of four different configurations at the exit of a single-screw extruder on the induction of beta phase in PP for four different rotational speeds. The configuration of a breaker plate with 120 orifices of 1-mm diameter and 7-mm length each, give the highest content of beta-phase (56.92%), for a screw rotational speed of 20 rpm. It was due to the shear caused separation of the melt when it passes through the orifices of the breaker plate. The breaker plate of configuration 4 (breaker plate with the greatest number of orifices) provided the largest number of contacts between the melt and the orifice walls resulting in chain alignment. The results show that the beta-phase can be induced in the polymer without any further additives, especially without any nucleating agents, but rather by using a special breaker plate configuration at the exit of the single-screw extruder. The skin-core structure of the polymer was only developed with one type of extruder configuration. © 2013 Wiley Periodicals, Inc. *J. Appl. Polym. Sci.* 130: 2932–2937, 2013

KEYWORDS: extrusion; crystallization; X-ray

Received 30 December 2012; accepted 3 May 2013; Published online 13 June 2013

DOI: 10.1002/app.39498

INTRODUCTION

Polypropylene (PP) is the choice polymer for home appliances, packaging and automotive industry due to its mechanical properties, simplicity of processing, the ability to incorporate varied types of fillers, and relative low cost.¹ It is well known that PP exhibits several crystalline forms, namely the monoclinic alpha-phase, the hexagonal beta-phase, and the orthorhombic gamma-phase.^{2–4} Among all crystal structures, the alpha-phase, obtained under ordinary industrial processing conditions, is the most stable. The presence of beta-phase improves mechanical properties of PP, such as increasing the impact strength and the elongation at break.^{1,5,6} It has been shown that the beta-phase of polypropylene could be formed under specific conditions, for example, by shear forces in controlled flow fields,^{7–9} by temperature gradients,¹⁰ in the presence of specific nucleating agents,^{11,12} and by using micron and nanometer scale fillers.^{13,14}

Many studies have been centered mainly on the formation of the beta-phase in PP in injection molding.^{15–20} Little attention,

however, has been given to the study of the beta-phase formation in extrusion, which is the main operation for the transformation of polymers. Duffo et al.²¹ have observed the presence of the beta-phase in samples obtained by cast film extrusion. These authors studied the effect of the roll temperature on the structure and morphology within the films. A high concentration of beta-phase in the outer sections was observed. Dragaun et al.⁸ reported the induction of beta-phase in PP by shear, during the processing of pipelines; however, these authors did not quantify the required shear rate or the beta-phase content.

In a previous article,²² we reported the possibility of inducing the beta-phase in PP with a small modification at the exit of the single screw extruder. The higher level of beta-phase with the use of a breaker plate was attributed to the shearing effect and to the subsequent orientation of the polymer chains in the orifices of the breaker plate. Therefore, the purpose of this article is to continue this study and to, mainly, investigate the effect of different configurations of the breaker plate, on the induction

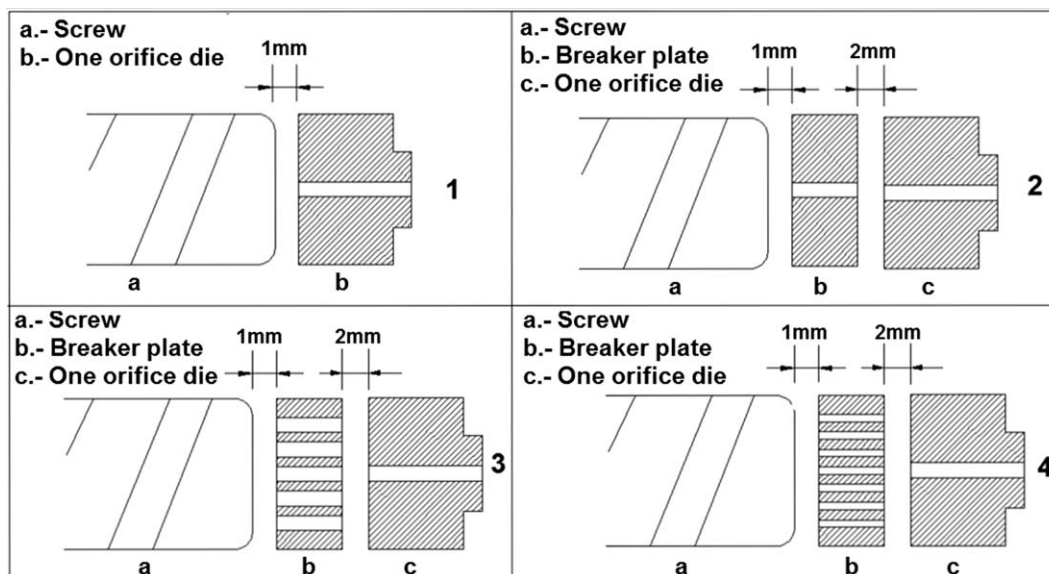


Figure 1. Configurations at the exit of the extruder (1) one orifice die of 3 mm in diameter and 23 m in length, (2) one orifice die and a breaker plate with 1 orifice of 2 mm in diameter and 12 mm in length, (3) one orifice die and a breaker plate with 19 orifices of 2 mm in diameter and 7 mm in length, (4) one orifice die and a breaker plates with 120 orifices of 1 mm in diameter and 7 mm in length.

of the beta-phase in PP. The cost of a breaker plate is very low and the construction is very simple. In the case of obtention of beta phase using specific additives, nucleating agents or fillers leads to a more expensive process by continuous consumption of chemical compounds.

EXPERIMENTAL

Materials and Sample Preparations

The polymer used in this study was a PP homopolymer resin (XH1760), supplied by Indelpro (Mexico). Its melt flow index is

3 g/10 min (230°C/2.16 kg), calculated according to ASTM D1238. The material was a commercially stabilized polymer without any further additives, especially without nucleating agents.

A 19-mm single-screw extruder (Beutelspacher, México) was used to conduct the experiments. The temperature profile ranged from 190°C in the feed section to 210°C at the die. Four different configurations at the exit of the extruder were used as shown in Figure 1. The first configuration (conf. 1) consisted of a one orifice die of 3-mm diameter and 23-mm length (Fig. 1). The second configuration (conf. 2) consisted of a one orifice die and a breaker plate with 1 orifice of 2 mm diameter and 12-mm length (Fig. 2). The third configuration (conf. 3)

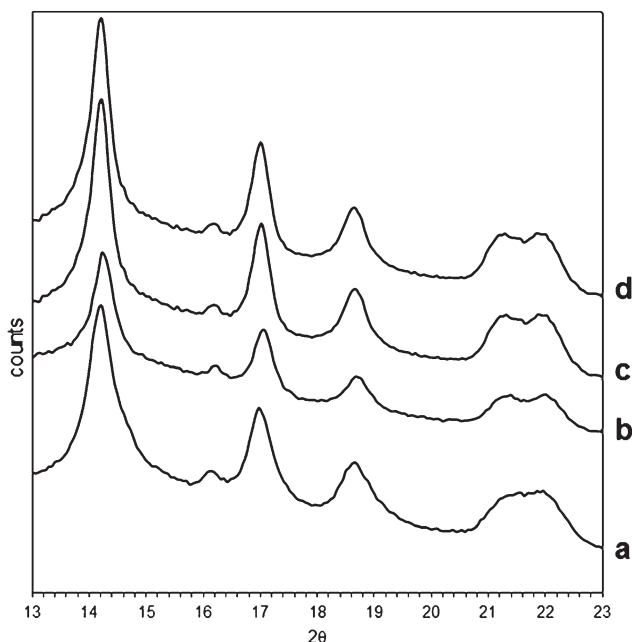


Figure 2. WAXD patterns of the samples obtained in the extruder with configuration 1 and with natural cooling process, (a) 20 rpm, (b) 40 rpm, (c) 60 rpm, (d) 80 rpm.

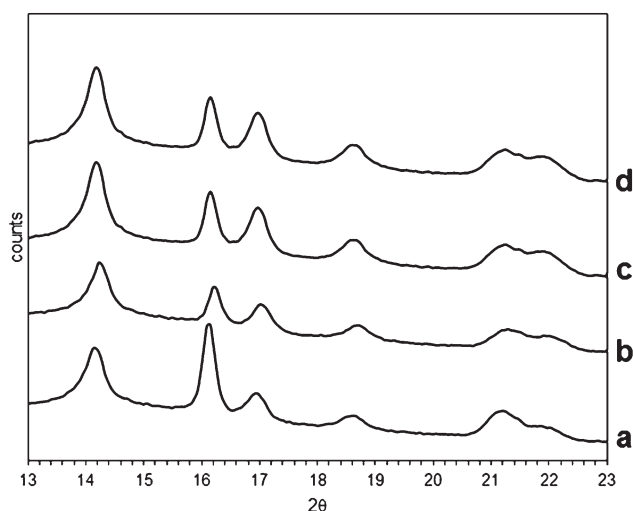


Figure 3. WAXD patterns of the samples obtained in the extruder with configuration 2 and with natural cooling process, (a) 20 rpm, (b) 40 rpm, (c) 60 rpm, (d) 80 rpm.

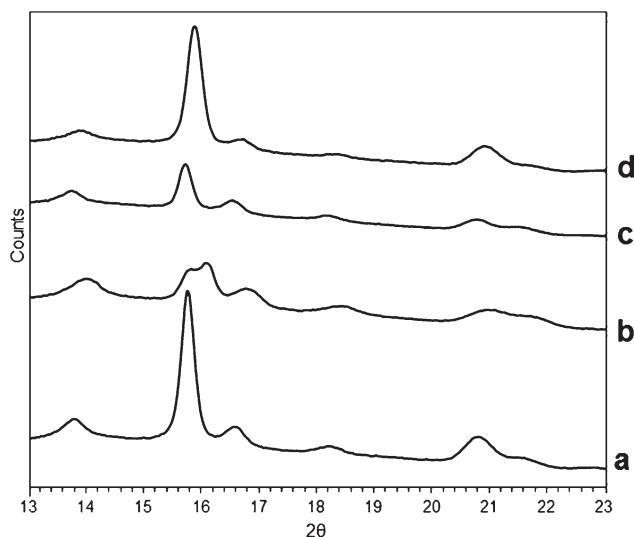


Figure 4. WAXD patterns of the samples obtained in the extruder with configuration 3 and with natural cooling process, (a) 20 rpm, (b) 40 rpm, (c) 60 rpm, (d) 80 rpm.

consisted of a one orifice die and a breaker plate with 19 orifices of 2-mm diameter and 7-mm length each (Fig. 3). The fourth configuration (conf. 4) consisted of a one orifice die and a breaker plate with 120 orifices of 1-mm diameter and 7-mm length each (Fig. 1).

The experiments were carried out at four different screw rotational speeds: 20, 40, 60, and 80 rpm. For each rotational speed the flow rate was measured at the exit of the extruder. For this, the extruder stayed working continuously for a period of 5 min, deemed sufficient to attain a steady temperature profile in the barrel, and at the exit of the extruder. After this stabilization period, samples ranging between 10 and 50 g in weight, depending on the screw rotational speed, were collected, at the exit of the extruder, in aluminum plates, during 2 min intervals. The weight of three samples, for each rotational speed, was averaged and the mass flow rate was converted to volumetric flow rate (Q).

The collected samples, at the exit of the extruder, were cooled down to room temperature with a cooling rate of $23^{\circ}\text{C}/\text{min}$ (natural cooling process), in the temperature range of $150\text{--}95^{\circ}\text{C}$, where primary crystallization occurs.

Table I. Flow Parameters for the Single Screw Extruder Configurations

Screw rotational speed (rpm)	Q (cm^3/s)	Shear rate at the orifice wall for the each orifice of the:				Residence time in each orifice of the:			
		Conf. 1 (s^{-1})	Breaker plates of the Conf. 2 (s^{-1})	Breaker plates of the Conf. 3 (s^{-1})	Breaker plates of the Conf. 4 (s^{-1})	Conf. 1 (s)	Breaker plates of the Conf. 2 (s)	Breaker plates of the Conf. 3 (s)	Breaker plates of the Conf. 4 (s)
20	0.10	37.74	63.66	6.70	8.35	1.63	0.38	3.8	6.70
40	0.20	75.47	140.06	13.40	16.70	0.81	0.19	1.9	3.35
60	0.30	113.21	280.11	20.10	25.05	0.54	0.13	1.26	2.23
80	0.40	150.94	420.17	26.81	33.40	0.41	0.09	0.95	1.67

Wide Angle X-Ray Diffraction (WAXD)

WAXD patterns were taken on a Philips X-pert diffractometer with the $\text{CuK}\alpha$ radiation at room temperature. Radial scans of intensity versus diffraction angle (2θ) were recorded ranging from 5° to 35° . Thin films of $20\text{--}30\ \mu\text{m}$ of the extrudate were sectioned normal to the extrusion direction, with a microtome, for analysis.

Optical Polarized Light Microscopy

To study the obtained structure and morphology of the PP extrudates, an Olympus optical microscope with a cross polarizer was used. For these tests thin films, similar to those for WAXD experiments, were inspected.

RESULTS AND DISCUSSION

The apparent shear rate ($\dot{\gamma}$, in s^{-1}) at the wall of each orifice was calculated using the following equation²³:

$$\dot{\gamma} = (4 \times Q_o) / (\pi \times R^3)$$

where, $Q_o = Q$ for one orifice die and breaker plate with one orifice; $Q_o = Q/19$ for each orifice of the breaker plate with 19 orifices and $Q_o = Q/120$ for each orifice of the breaker plate with 120 orifices; Q is the extruder volumetric flow rate in cm^3/s , and R is the radius of the orifice.

The residence time in each orifice of the one orifice die as well as in each orifice of the breaker plate was calculated as:

$$t_{\text{res}} = V / Q_o$$

where, V is the volume of the orifice in cm^3 .

For the calculations, it was assumed that there is no stagnation in the flow from the end of screw to the exit of extruder. The obtained shear rate and residence time values for the four configurations are shown in Table I.

The WAXD patterns for the samples obtained in the extruder with configurations 1, 2, 3, and 4, for the four different screw rotational speeds, are shown in Figures 2–5, respectively. The ordinary WAXD patterns of the PP show the diffraction peaks at the 2θ angles of 14.1° , 16.9° , and 18.5° , corresponding to the crystal planes (110), (040), and (130), respectively. The beta crystalline form is known to exhibit a strong peak at a 2θ angle of 16° corresponding to the crystal plane (300).²⁴ The relative content of beta-phase (K) can be calculated according to the Turner-Jones equation²⁴:

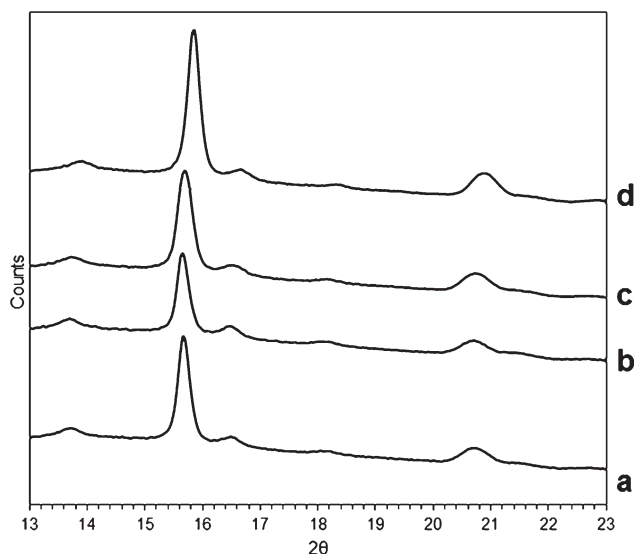


Figure 5. WAXD patterns of the samples obtained in the extruder with configuration 4 and with natural cooling process (a) 20 rpm, (b) 40 rpm, (c) 60 rpm, (d) 80 rpm.

$$K = H_{\beta} / [H_{\beta} + (H_{\alpha 1} + H_{\alpha 2} + H_{\alpha 3})]$$

where H_{β} is the height of the strong single beta-form peak (300), and $H_{\alpha 1}$, $H_{\alpha 2}$, and $H_{\alpha 3}$ are the heights of the three strong equatorial alpha-form peaks (110), (040), and (130), respectively. The obtained K values for the extruded samples through configurations 1, 2, 3, and 4 and for the four rotational speeds are presented in Table II.

Table II. Beta-Phase Content (K)

Screw rotational speed	Conf. 1 (%)	Conf. 2 (%)	Conf. 3 (%)	Conf. 4 (%)
20	16.8	38.09	53.42	56.92
40	21.74	25.97	28.57	40.85
60	19.69	25.82	36.47	40.31
80	20.51	25.6	40	42.19

The results in Table II clearly show that, for samples obtained at the end of the extruder, the one orifice die of 3-mm diameter and 23-mm length plus a breaker plate with 120 orifices of 1 mm diameter and 7-mm length (configuration 4) yielded higher PP beta-phase content than that with the die alone (configuration 1). The increase in the beta-phase content was sharpest at the rotational speed of 20 rpm, 40.12%, followed by smaller increases: 19.11, 20.62, and 21.68% for the other rotational speeds of 40, 60, and 80 rpm, respectively. These results demonstrate that the use of a breaker plate increases the beta phase contents of the extrudates, as was reported in a previous work.²² However, the results show that with configuration 4 the beta phase content was the highest, although in this configuration 4 the shear rate values are not the highest. This means that there is another effect that influences the formation of beta phase in the samples passing through the breaker plate.

According to Newton,²⁵ the shear rate is the velocity by which the parts of the fluid are being separated. This process of fluid separation produces an alignment of the macromolecules in a form of fibrillar bundles along the flow direction during its

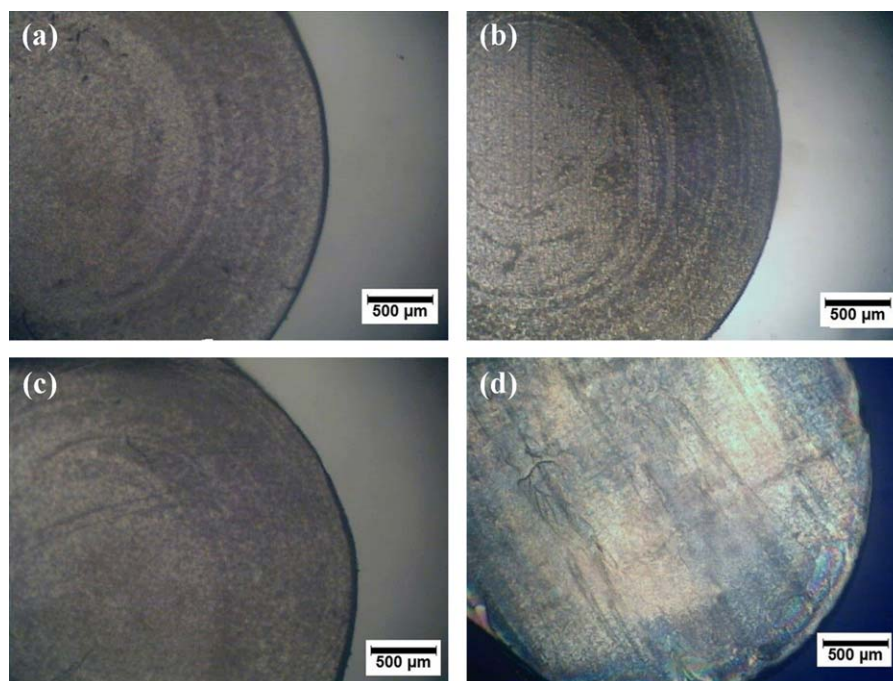


Figure 6. Micrographs obtained by polarized light optical microscopy of the samples obtained in the extruder with configuration 2 and with natural cooling process: (a) 20 rpm, (b) 40 rpm, (c) 60 rpm, (d) 80 rpm. [Color figure can be viewed in the online issue, which is available at wileyonlinelibrary.com.]

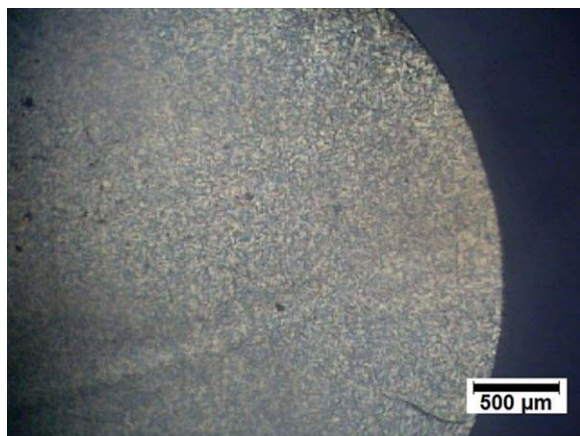


Figure 7. Micrographs obtained by polarized light optical microscopy of the samples obtained in the extruder with configuration 4, for rotational speed of 20 rpm and with natural cooling process. [Color figure can be viewed in the online issue, which is available at wileyonlinelibrary.com.]

passage through the breaker plate. The preoriented molecules crystallize easily and act as row-nuclei which generate supermolecular structure. This supermolecular structure is generally rich in the beta-modification of iPP. Therefore, the higher beta-phase content obtained in the samples extruded by configuration 4, which has a breaker plate with a larger number of orifices (120), is due to the process of separation of the fluid and thus the alignment of macromolecules takes place in a greater volume of sample. The breaker plate with the greatest number of orifices provides the largest number of contacts between the melt and the orifice walls resulting in chain alignment that favored the formation of beta spherulites in these zones.⁸

Conversely, some authors^{26,27} reported that the supermolecular structure generated in the melt under shear has a peculiar cylindrical symmetry. This supermolecular cylindrical structure in microtomed sections from the extrudate in the machine direction shows a skin-core structure. This skin-core structure reveals that the sheared region consists of alpha-cylindrites oriented in the machine direction and the surrounding region is generally rich in partially oriented beta type spherulites.

Only in samples, obtained using a one orifice die of 3-mm diameter and 23-mm length, as well as, a breaker plate with 1 orifice of 2-mm diameter and 12-mm length (configuration 2 in Fig. 1), and for the four rotational speeds, a skin-core structure can be observed, as shown in the micrographs of Figure 6. In the samples obtained by the other configurations (1, 3, and 4) no skin-core structure was observed. This can be seen in Figure 7 which shows, as an example, the micrograph for a naturally cooled sample, obtained by configuration 4 and a rotational speed of 20 rpm.

In configuration 2, the mixture passes through two holes, one of the breaker plate and the other of the die. This produces a great alignment of the chains in the melt, compared with configuration 1. As the diameter of the breaker plate orifice is smaller than that of the die it gives rise to higher shear rate

(Table I), which leads to the formation of the skin-core structure, and hence the induction of beta-phase content. However, even though in configurations 3 and 4 the melt is sheared and aligned during its passage through the breaker plate, it is again brought together just before the orifice of the die, which produces the loss of the skin-core structure.

CONCLUSIONS

The beta-phase induction in polypropylene in a single-screw extruder was achieved without any special additive or nucleating agents and by using a breaker plate at the exit of the extruder. Four different breaker plates were studied. Configuration 4 with a one orifice die and a breaker with the greatest number of orifices (120), gives the highest beta-phase contents at all screw rotational speeds used. This behavior was correlated to the process of separation and alignment of the melt when it passes through the orifices of the breaker plate. These results show the possibility of inducing the beta-phase in PP employing a breaker plate at the exit of the single screw extruder which reduces the cost at the industrial level due to elimination of any type of nucleating agent or mineral filler to enhance the content of this phase.

ACKNOWLEDGMENTS

The authors are grateful to M.Sci Sebastian Pacheco Buendia (Centro de Investigación en Ciencia Aplicada y Tecnología de Avanzada del IPN, Unidad Altamira) for the technical assistance and to CONACYT (Mexico) for the student-scholarship No 213733.

REFERENCES

1. Tjong, S. C.; Li, R. K. Y.; Cheung, T. *Polym. Eng. Sci.* **1997**, *37*, 166.
2. Keith, H. D.; Padden, F. J.; Walter, N. M.; Wycoff, M. W. *J. Appl. Phys.* **1959**, *30*, 1485.
3. Brückner, S.; Meille, S. V. *Nature* **1989**, *340*, 455
4. Meille, S.V.; Bruckner, S.; Porzio, W. *Macromolecules* **1990**, *23*, 4114.
5. McGenity, P. M.; Hooper, J. J.; Paynter, C. D.; Riley, A. M.; Nutbeem, C.; Elton, N. J.; Adams, J. M. *Polymer* **1992**, *33*, 5215.
6. Tjong, S. C.; Shen, J. S.; Li, R. K. Y. *Polym. Eng. Sci.* **1996**, *36*, 100
7. Farah, M.; Bretas, R. E. S. *J. Appl. Polym. Sci.* **2004**, *91*, 3528.
8. Dragaun, H.; Hubeny, H.; Muschik, H. *J. Polym. Sci. Polym. Phys. Ed.* **1977**, *15*, 1779.
9. Somani, R. H.; Hsiao, B. S.; Nogales, A.; Fruitwala, H.; Srinivas, S.; Tsou, A. H. *Macromolecules* **2001**, *34*, 5902.
10. Lovinger, A. J.; Chua, J. O.; Gryte, C. C. *J. Polym. Sci. Polym. Phys. Ed.* **1977**, *15*, 641.
11. Jacoby, P.; Bersted, B. H.; Kissel, W. J.; Smith, C. E. *J. Polym. Sci. Polym. Phys. Ed.* **1986**, *24*, 461.
12. Shi, G.; Zhang, X. *Thermochim. Acta* **1992**, *205*, 235.

13. Liu, J.; Wei, X.; Guo, Q. *J. Appl. Polym. Sci.* **1990**, *41*, 2829.
14. Medellín, F. J.; Mata, J. M.; Hsiao, B. S.; Waldo, M. A.; Ramírez, E.; Sánchez, S. *Polym. Eng. Sci.* **2007**, *47*, 1889.
15. Cermak, R.; Obadal, M.; Ponizil, P.; Polaskova, M.; Stoklasa, K.; Lengalova, A. *Eur. Polym. J.* **2005**, *41*, 1838.
16. Fitchmun, D. R.; Mencik, Z. *J. Polym. Sci. Polym. Phys. Ed.* **1973**, *11*, 951.
17. Murphy, M. W.; Thomas, K.; Bevis, J. M. *Plast. Rubb. Process. Appl.* **1988**, *9*, 3.
18. Fujiyama, M. *Int. Polym. Process.* **1992**, *7*, 84.
19. Rybnikar, F. *J. Appl. Polym. Sci.* **1989**, *38*, 1479.
20. Kotek, J.; Keinar, I.; Baldrian, J.; Raab, M. *Eur. Polym. J.* **2004**, *40*, 679.
21. Duffo, P.; Monasse, B.; Haudin, J. M. *Int. Polym. Process.* **1990**, *5*, 272.
22. Lozano, T.; Laria, J.; Lafleur, P.; Sanchez-Vargas, S.; Rodriguez-Gonzalez, F.; Morales-Cepeda, A. B. *Polym. Eng. Sci.* **2012**, *52*, 1672.
23. Macosko, C. W. *Rheology Principles Measurements and Applications*; Wiley-VCH: New York, **1998**.
24. Turner-Jones, A.; Aizlewood, J. M.; Beckett, D. R. *Makromol. Chem.* **1964**, *75*, 134.
25. Reiner, M. *Deformation, Strain and Flow*; Wiley-Interscience: New York, **1960**.
26. Varga, J.; Karger-Kocsis, J. *J. Polym. Sci. Part B. Polym. Phys.* **1996**, *34*, 657.
27. Varga, J. *J. Mater. Sci.* **1992**, *27*, 2557.